Journal of Pathology
J Pathol 2016; **240:** 425–436
Published online 21 October 2016 in Wiley Online Library (wileyonlinelibrary.com) DOI: 10.1002/path.4782

ORIGINAL PAPER

Propionibacterium acnes overabundance and natural killer group 2 member D system activation in corpus-dominant lymphocytic gastritis

Ana Montalban-Arques,[1,2] Philipp Wurm,[1,2] Slave Trajanoski,[3] Silvia Schauer,[1] Sabine Kienesberger,[4,5] Bettina Halwachs,[1,2,5] Christoph Högenauer,[2,6] Cord Langner[1] and Gregor Gorkiewicz[1,2,5,*]

[1] *Institute of Pathology, Medical University of Graz, Graz, Austria*
[2] *Theodor Escherich Laboratory for Medical Microbiome Research, Medical University of Graz, Graz, Austria*
[3] *Centre for Medical Research, Medical University of Graz, Graz, Austria*
[4] *Institute of Molecular Biosciences, University of Graz, Graz, Austria*
[5] *BioTechMed, Interuniversity Cooperation, Graz, Austria*
[6] *Department of Internal Medicine, Division of Gastroenterology and Hepatology, Medical University of Graz, Graz, Austria*

**Correspondence to: G Gorkiewicz, Institute of Pathology; Medical University of Graz, Auenbruggerplatz 25, 8036 Graz, Austria. E-mail: gregor.gorkiewicz@medunigraz.at*

Abstract

Corpus-dominant lymphocytic gastritis (LyG) is characterized by CD8$^+$ T-cell infiltration of the stomach epithelium by a so far uncharacterized mechanism. Although *Helicobacter pylori* is typically undetectable in LyG, patients respond to *H. pylori* antibiotic eradication therapy, suggesting a non-*H. pylori* microbial trigger for the disease. Comparative microbiota analysis of specimens from LyG, *H. pylori* gastritis and healthy controls precluded involvement of *H. pylori* in LyG but identified *Propionibacterium acnes* as a possible disease trigger. In addition, the natural killer group 2 member D (NKG2D) system and the proinflammatory cytokine interleukin (IL)-15 are significantly upregulated in the gastric mucosa of LyG patients, and gastric epithelial cells respond to microbe-derived stimuli, including live *P. acnes* and the microbial products short-chain fatty acids, with induction of NKG2D ligands. In contrast, *H. pylori* infection does not activate or even repress NKG2D ligands. Together, our findings identify *P. acnes* as a possible causative agent for LyG, which is dependent on the NKG2D system and IL-15 activation.

Keywords: lymphocytic gastritis; 16S rRNA gene; stomach microbiota; *Propionibacterium acnes*; *Helicobacter pylori*; intraepithelial lymphocytes; NKG2D; MICA; IL-15; short-chain fatty acids; gastric epithelial cells

Received 9 March 2016; Revised 15 July 2016; Accepted 9 August 2016

No conflicts of interest were declared.

Introduction

Lymphocytic gastritis (LyG) accounts for up to 4.5% of chronic gastritis cases [1]. Clinical symptoms range from abdominal pain and dyspepsia to severe cases with protein-losing gastroenteropathy, weight loss, and anaemia [2]. LyG is characterized histologically by an increased abundance of CD8$^+$ intraepithelial lymphocytes (IELs), namely 25 per 100 epithelial cells (ECs) in the gastric epithelium (normal range <8 per 100 ECs). These IELs typically show a cytotoxic phenotype with granzyme B and T-cell intracellular antigen-1 expression [3,4]. Initially reported in the context of 'varioliform gastritis', LyG seems to be a histopathological syndrome rather than a single disease [1]. Up to 45% of LyGs are associated with coeliac disease (CeD). In these cases, intraepithelial lymphocytosis is normally dominant in the gastric antrum. Several cases are thought to have been associated with *Helicobacter pylori* infection, although *H. pylori* is often not detectable [5]. Rare causes include Crohn's disease, human immunodeficiency virus infection, common variable immunodeficiency, or the use of ticlopidine [2]. Nevertheless, >20% of cases have an unknown aetiology, not associated with the above-mentioned conditions. Interestingly, antibiotic therapy, namely *H. pylori* eradication therapy, seems to be an effective treatment for LyG, even in the absence of identifiable *H. pylori*, suggesting an alternative bacterial cause for the disease [6–8].

The molecular causes triggering the massive CD8$^+$ IEL infiltration in LyG are also unknown. In CeD, the natural killer group 2 member D (NKG2D) system is critical for recruitment of CD8$^+$ IELs and subsequent villus atrophy in the duodenum [9,10]. Natural killer (NK) cells, CD8$^+$ T cells, γδ T cells, NKT

cells and certain subsets of $CD4^+$ T cells express the NKG2D receptor [11]. The NKG2D receptor ligands (NKG2DLs) are expressed mainly on ECs at low levels under physiological conditions, but their expression is induced under conditions of cell stress, such as viral infection, neoplastic transformation, heat shock, or gliadin challenge [9,10,12–14]. In humans, NKG2DLs include major histocompatibility complex (MHC) class I chain-related protein A (MICA), MHC class I chain-related protein B (MICB), and up to six different UL16-binding proteins (ULBPs), also known as RAET1 proteins [11,15]. Upon ligand–receptor interaction, NKG2D triggers a cytotoxic response in the receptor-bearing lymphocyte, eliminating the stressed cell that is overexpressing the ligand. This reaction is enhanced by the presence of the proinflammatory cytokine interleukin (IL)-15 [9,16]. Recently, it has been demonstrated that NKG2DL expression in the gastrointestinal (GI) mucosa is modulated by the gut microbiota [17]. Moreover, short-chain fatty acids (SCFAs) such as propionate and butyrate, which represent microbiota-derived products, are potent inducers of NKG2DLs [18].

In the current study, we aimed to identify a possible bacterial trigger for LyG development by employing comparative microbiota analysis of stomach specimens obtained from persons with LyG, *H. pylori* gastritis (HpG), and healthy controls. Moreover, expression analysis of the NKG2D–NKG2DL system and the proinflammatory cytokine IL-15 was used to assess activation of these molecular determinants that are needed for IEL infiltration. Finally, cell culture experiments were used to test whether gastric ECs are able to respond to microbial stimuli, including live *Propionibacterium acnes*, *H. pylori*, and the microbial products SCFAs, by induction of NKG2DLs.

Materials and methods

Ethics statement

The use of human tissue specimens was approved by the institutional review board of the Medical University of Graz (EK-23-212ex10/11).

Specimens, histology, and immunohistochemistry

Formalin-fixed paraffin-embedded (FFPE) biopsy specimens were derived from the files of the Institute of Pathology of the Medical University of Graz (supplementary material, Table S1). Only cases with paired duodenal, gastric antral and gastric corpus specimens were included in the study. *H. pylori* carriage was determined by Warthin–Starry staining [19] and/or immunohistochemistry with an anti-*H. pylori* antibody (clone SP48; Ventana, Tucson, AZ, USA). The following entities were used: healthy corpus ($n = 24$), corpus biopsies from corpus-dominant LyG with proven absence of CeD (denoted LyG, $n = 25$), and corpus biopsies of H. pylori gastritis (denoted HpG, $n = 25$). Metadata and analyses performed on specimens are provided in supplementary material, Table S1. Sections from FFPE tissue specimens were stained with monoclonal mouse anti-human CD8 (clone C8/144B; dilution 1:30; Dako Glostrup, Denmark), monoclonal mouse anti-human CD4 (clone 4B12; dilution 1:20; Labvision, Fremont, CA, USA) and MICA/B (clone F-6; dilution 1:200; Santa Cruz Biotechnology, Dallas, TX, USA) antibodies, according to the supplier's recommendations.

Microbiota analysis

DNA extraction for microbiota analysis is described in Supplementary materials and methods. DNA quality and concentration were determined spectrophotometrically with a NanoDrop ND-3300 instrument and the PicoGreen assay (Thermo Fisher Scientific, Waltham, MA, USA). Only specimens yielding an absorbance ratio of >0.8 at 260/280 nm and an absorbance ratio of ~2 at 260/230 nm, respectively, were considered for further analyses. For amplification of the bacterial 16S rRNA gene FLX one-way fusion primers (Lib-L kit, Primer A, Primer B; Roche 454 Life Science, Branford, CT, USA) with the template-specific sequence F27 and R357 (supplementary material, Table S2) targeting the V1–2 region of the 16S rRNA gene were used (amplicon length of 349 bp). Primers were chosen on the basis of their performance, enabling superior community capture and taxonomic resolution [20], and their good polymerase chain reaction (PCR) performance when applied to FFPE samples. PCR amplification was performed as described previously [21]. Reactions for each sample were performed in triplicate, the quality of amplification products was checked visually on agarose gels, and only specimens resulting in reliable PCR amplification were used further. Amplicons were gel-purified, pooled, and sequenced with the GS FLX Titanium Sequencing Kit XLR70 (Roche 454 Life Science), as described previously [21]. For microbiota analysis, raw files from 454 FLX pyrosequencing were processed with MOTHUR v.1.31.2 according to the standard 454 SOP of MOTHUR [22]. Sequencing errors were reduced with MOTHUR's implementation of PyroNoise [23], and the command pre.cluster [24] was used to remove sequences that arose because of pyrosequencing errors. Chimeras were removed with UCHIME [25], and non-bacterial contaminants were removed by use of the Ribosomal Database Project (RDP) reference [26]. The high-quality reads were aligned to the SILVA database [27,28]. For operational taxonomic unit (OTU)-based analyses, the processed fasta files from MOTHUR were introduced into QIIME v.1.7.0 [29]. OTUs were formed by clustering the sequences with uclust [30], with a similarity score of 97% (OTU 97% identity), and taxonomy was assigned by using the RDP classifier and Greengenes reference OTUs. A *de novo* OTU picking strategy was employed. The biomarker discover program LEfSe (linear discriminant analysis effect

size) was used to determine differentially abundant OTUs [31]. A batch file specifying the parameters used for microbiota analyses is given in Supplementary materials and methods. Differences in alpha-diversity measures were tested by one-way ANOVA and a *post hoc* Bonferroni test. Principal coordinate analysis (PCoA) plots were created on the basis of a weighted-unifrac [32] distance matrix, and statistical differences between groups were calculated with ANOSIM. The presented values are always mean ± standard error of the mean if not indicated otherwise.

Reverse transcription quantitative PCR (RT-qPCR)

Total RNA from FFPE samples (10 sections, each 5 µm in thickness) was isolated with deparaffinization solution (Qiagen, Hilden, Germany) and the RNeasy FFPE kit, which includes a DNase treatment step (Qiagen). RNA from cell culture experiments was extracted by the use of TRIzol (Thermo Fisher Scientific) and the PureLink RNA mini kit (Invitrogen), according to the manufacturer's specifications. RNA quality and quantity were determined spectrophotometrically by the use of a NanoDrop instrument (ThermoScientific), as described above, and 1 µg of total RNA was used for cDNA synthesis with the GeneAmp RNA PCR kit (Thermo Fisher Scientific), according to the manufacturer's instructions. Quantitative real-time PCR was performed with an ABI PRISM 7900HT instrument (Applied Biosystems) and SYBR Green PCR core reagents (Applied Biosystems). The oligonucleotide primers used are shown in supplementary material, Table S2. Reaction mixtures were incubated for 10 min at 95 °C, and this was followed by 40 cycles of 15 s at 95 °C, 1 min at 60 °C, and finally 15 s at 95 °C, 15 s at 60 °C, and 15 s at 95 °C. For each mRNA target, the expression level was normalized by using the β-actin gene (*ACTB*) as a reference, and ratios were calculated with Pfaffl's method [33]. For determination of *P. acnes* loads, 50 ng of total DNA extracted from the FFPE specimens was used as a normalized input for real-time PCR amplification. Each PCR reaction was performed in triplicate, and analyses were repeated three times.

Bacterial culture

P. acnes strains originating from the human stomach were kindly provided by B Mayo [34], and cultured under anaerobic conditions (Genbox anaer; bioMerieux, Marcy l'Etoile, France) on Columbia blood agar plates (bioMerieux) at 37 °C. *H. pylori* strains PMSS1 [35] and SS1 [36] were routinely grown on Columbia blood agar plates at 37 °C for 3 days in a microaerobic atmosphere (Genbox microaer; bioMerieux) prior to gastric cell line infection. *Escherichia coli* DSM30083 (purchased from DSMZ, Braunschweig, Germany) and *E. coli* DH5α [37] were cultured routinely on Columbia agar plates (bioMerieux) under aerobic conditions at 37 °C.

Cell culture, infection, and SCFA stimulation assays

AGS cells were obtained from Cell Lines Service (Eppelheim, Germany). MKN28 cells were originally obtained from the Japanese Collection of Research Bioresources (JCRB; http://cellbank.nibio.go.jp/) and were kindly provided by S Wessler [38]. Epithelial cells were seeded at 1.5×10^5 per well of six-well plates in 3 ml of Dulbecco's modified Eagle's medium (DMEM) high glucose (4.5 g/l) (GE Healthcare, Vienna, Austria), 10% fetal bovine serum (FBS) (Thermo Fisher Scientific) and 5 mM L-glutamine (PAA, Vienna, Austria), and were grown to 80% confluence in a water-saturated atmosphere of 95% air and 5% CO_2 at 37 °C. Prior to the infection assays, a single *E. coli* colony was transferred into a 15-ml tube containing 3 ml of Brucella broth (Roth, Karlsruhe, Germany), and incubated with gentle agitation (100 r.p.m.) at 37 °C for 4 h. For *P. acnes* infection, a bacterial suspension with an $OD_{600\,nm}$ of 0.1 [corresponding to 10^8 colony-forming units (CFUs)/ml] was cultivated for 24 h in wells of six-well plates containing 3 ml of DMEM high glucose (4.5 g/l), containing 10% FBS and 5 mM L-glutamine. Subsequently, AGS and MKN28 cells were infected with *P. acnes*, *H. pylori* or *E. coli* at a multiplicity of infection (MOI) of 1:50 for 24 h. Measurement of SCFAs in co-culture supernatants by gas chromatography–mass spectrometry is described in Supplementary materials and methods. For SCFA stimulation, cells (1.2×10^6/well) were incubated with 5 mM propionate, butyrate, acetate, or hydrochloric acid (Sigma Aldrich, St. Louis, MO, USA) for 4 h [39–41]. Subsequently, cells were harvested by gentle centrifugation 300 g, 2 min and stored in 500 µl of Trizol (Thermo Fisher Scientific) for RNA isolation. Cells used for protein expression were rescued after 4 h of stimulation with SCFAs in DMEM high glucose (10% FBS, 5 mM L-glutamine) for another 4 h before being analysed by flow cytometry [18]. Experiments were performed in triplicate and repeated three times.

Flow cytometry

AGS and MKN28 cells were harvested in ice-cold phosphate-buffered saline, because trypsin cleaves surface NKG2DLs, giving false-negative results [42]. A detailed protocol specifying the preparation steps for flow cytometry is given in Supplementary materials and methods.

Statistical analysis

Quantitative PCR and flow cytometry data were assessed with the D'Agostino & Pearson test for their normal distribution. Data are given as mean ± standard deviation if not otherwise specified. Statistical analyses were performed with GraphPad Prism 5 software, by the use of one-way ANOVA and either Tukey's *post hoc* test (for FFPE samples) or Dunnett's *post hoc* test (for *in vitro* and flow cytometry assays). *p*-Values of <0.05 were considered to be statistically significant.

Data deposition

The sequencing data generated for this work can be accessed via the EBI short read archive (EBI SRA) under the accession number ERP013255.

Results

LyG is not associated with *H. pylori* infection but is signified by *P. acnes* overabundance

To investigate the gastric microbiota in LyG and to discern a possible bacterial disease trigger, we subjected gastric corpus biopsies originating from LyG ($n = 13$), HpG ($n = 5$) and healthy controls ($n = 6$) to comparative 16S rRNA gene profiling; 4841 ± 2309 reads were generated per sample, corresponding, on average, to 74 ± 28 OTUs (97% identity) per sample. Microbial richness, which is a measure of how many taxa are detectable in the respective sample, showed no difference between entities (Figure 1A). In contrast, diversity and evenness, which are measures of how diverse a microbial community is and how equally the taxa therein are distributed, were significantly lower in HpG and LyG than in controls (Figure 1B; supplementary material, Table S3). This finding suggests that, in LyG, similarly to HpG, certain bacteria may dominate the microbial community. PCoA (measure: weighted unifrac distance) indicated significantly different microbial community structures (ANOSIM, $p < 0.001$) of entities (Figure 1C). Comparative analysis with LEfSe revealed certain significantly different abundant phylotypes in entities (supplementary material, Table S4). Importantly, only two OTUs showed a markedly high linear discriminant analysis (LDA) score (LDA of >5.1) and statistical significance. *H. pylori* OTU527 showed significantly increased abundance in HpG ($p = 0.0003$), and *P. acnes* OTU133 showed significantly increased abundance in LyG ($p < 0.0006$; Figure 1D). *P. acnes* accounted for $47.36 \pm 2.74\%$ of taxa in LyG, $22.23 \pm 3.82\%$ in controls, and $24.77 \pm 5.63\%$ in HpG (Figure 1E). *H. pylori* accounted for $51.54 \pm 11.11\%$ of taxa in HpG, but was nearly absent in LyG and controls. Only one healthy control (specimen 13) and two LyG specimens (specimens 32 and 43) contained *H. pylori* at low abundance ($0.49 \pm 1.2\%$ and $0.18 \pm 0.62\%$, respectively). Low-level colonization of asymptomatic individuals with *H. pylori* has been described recently [43–46]. The taxonomic differences were also reflected at the phylum level, wherein HpG showed a significant relative increase in the abundance of proteobacteria ($55.91 \pm 8.45\%$); $89.95 \pm 7.22\%$ of proteobacterial reads originated from *H. pylori*. LyG showed a significant relative increase in the abundance of actinobacteria ($58.12 \pm 2.56\%$); $81.36 \pm 8.68\%$ of them were represented by *P. acnes*. Accordingly, the *Firmicutes* and *Bacteroidetes* were significantly depleted in HpG and LyG as compared with controls (Figure 1F; supplementary material, Figure S1). Finally, quantitative PCR performed on LyG, HpG and controls confirmed significantly increased *P. acnes* loads in LyG (Figure 1G). Moreover, a significant correlation of abundance determined by 16S next-generation sequencing and load determined by quantitative PCR was evident, validating the microbiota analysis results (supplementary material, Figure S2). Collectively, these data indicate that LyG is not associated with *H. pylori* infection, but shows significantly increased *P. acnes* loads.

The NKG2D–NKG2DL system is induced in LyG but not in HpG

The NKG2D–NKG2DL system and the proinflammatory cytokine IL-15 are major determinants for IEL recruitment in the gut. Upregulation of both factors leads to intraepithelial lymphocytosis, and subsequently to villus atrophy, in CeD [9,10]. The phenotypic similarities between LyG and CeD prompted us to investigate the involvement of this cell stress-sensing system in LyG. First, we comparatively assessed the number of $CD8^+$ and $CD4^+$ lymphocytes in gastric corpus specimens from LyG, HpG and healthy controls by immunohistochemistry (Figure 2A). LyG cases showed significant increases in the numbers of $CD8^+$ lymphocytes as compared with HpG and healthy controls (Figure 2B). These $CD8^+$ T cells were mainly IELs. The average $CD8^+$ IEL counts were 28.04 ± 4.15 per 100 ECs in LyG, 5.6 ± 0.62 per 100 ECs in healthy controls, and 4.64 ± 1.18 per 100 ECs in HpG (Figure 2C). In contrast, HpG showed a significant increase in the number of $CD4^+$ T cells [14.4 ± 5.65 in five high-power fields (HPFs)] as compared with healthy controls; the $CD4^+$ T cells were mainly present in the lamina propria (Figure 2A, B). Next, we comparatively assessed the expression of *NKG2D*, NKG2DLs (*MICA*, *MICB*, *ULBP1*, *ULBP2*, *ULBP3* and *ULBP4*) and *IL-15* by RT-qPCR. Gastric corpus biopsies of LyG showed significant overexpression of *NKG2D* and *IL-15* mRNA as compared with HpG and healthy controls, and *MICA* levels were significantly increased as compared with healthy controls (Figure 2D). *MICB*, *ULBP1* and *ULBP2* mRNA expression was slightly repressed in LyG (supplementary material, Figure S3). It is of note that HpG showed no significant induction of the expression of assessed markers, which correlated with the observed absence of $CD8^+$ T-cell infiltration in HpG (Figure 2B). Gastric corpus biopsies of LyG also showed pronounced staining with an MICA/B antibody in areas wherein the numbers of IELs were increased, indicating induction of the system in the epithelium (Figure 2E). Taken together, these data indicate that expression of the NKG2D–NKG2DL system and of the proinflammatory cytokine IL-15 are induced in LyG, suggesting that these factors are important for $CD8^+$ IEL recruitment and disease pathogenesis. Interestingly, NKG2D–NKG2DL system and IL-15 expression are not induced in HpG, pointing towards deviating mucosal immune reactions and pathogeneses of both diseases.

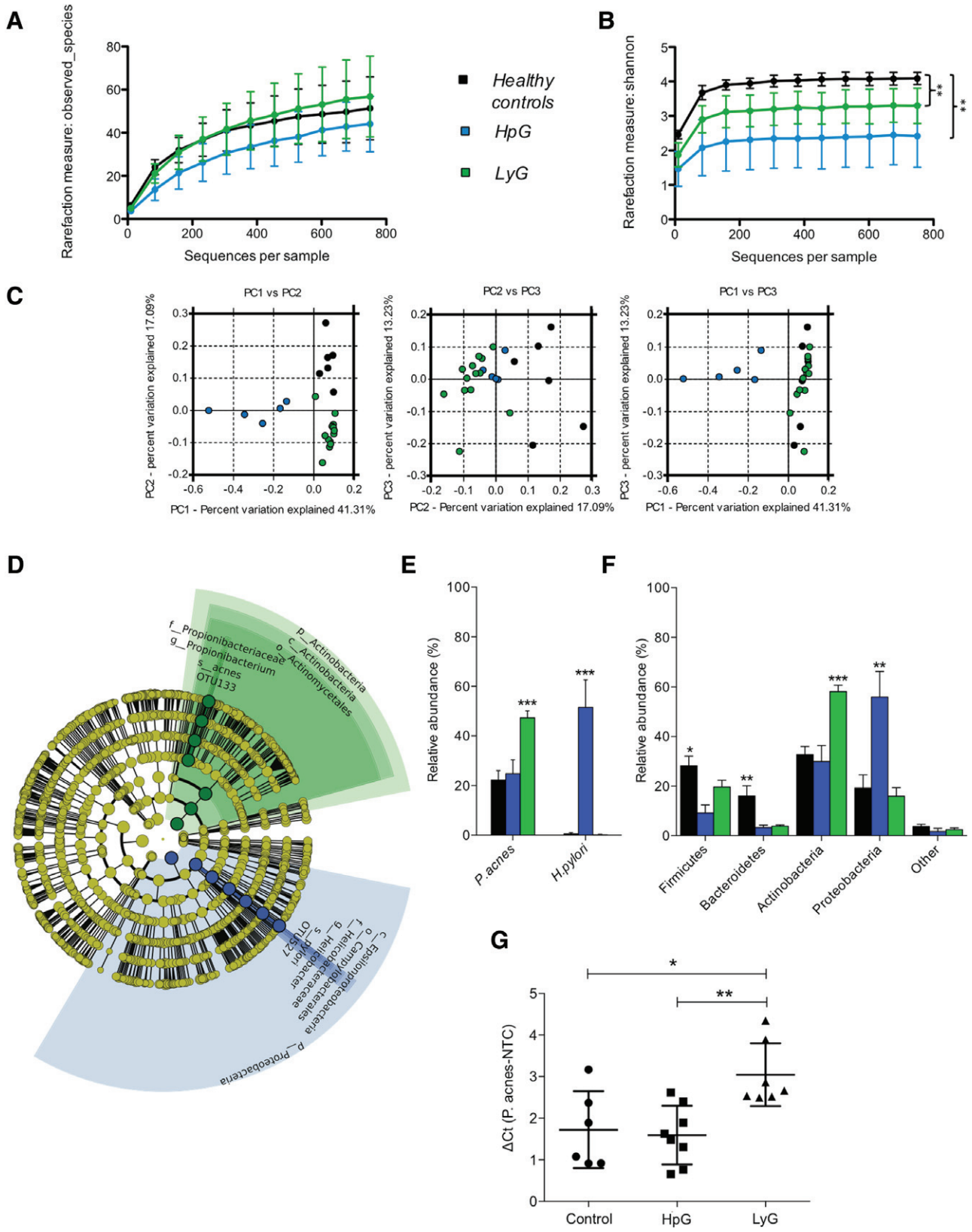

Figure 1. Comparative microbiota analyses of LyG, HpG and healthy controls. (A) Microbial richness (i.e. number of identifiable taxa) showed no statistically significant difference between entities. (B) The Shannon diversity index was significantly lower in HpG and LyG than in controls. (C) Significantly different microbial community structures in HpG, LyG and healthy controls, as indicated by distinct clustering in PCoA (measure: weighted unifrac; ANOSIM, $p < 0.001$). (D) Cladogram representing the LEfSe output comparing controls, HpG and LyG. Only two highly significant associations with entities (LDA score of >5.1) were found, namely *H. pylori* in HpG and *P. acnes* in LyG. The diameter of each circle is proportional to the taxon's abundance in the graph. (E) Relative abundance of *P. acnes* and *H. pylori* in healthy controls, HpG, and LyG. (F) Relative abundance of the main bacterial phyla in healthy controls, HpG samples, and LyG samples (*$p < 0.05$, **$p < 0.01$, ***$p < 0.001$; according to LEfSe analysis encompassing the Kruskal–Wallis and Wilcoxson tests). (G) Quantitative PCR results validating *P. acnes* overabundance in LyG (*$p < 0.05$; **$p < 0.01$; one-way ANOVA and Tukey's *post hoc* test).

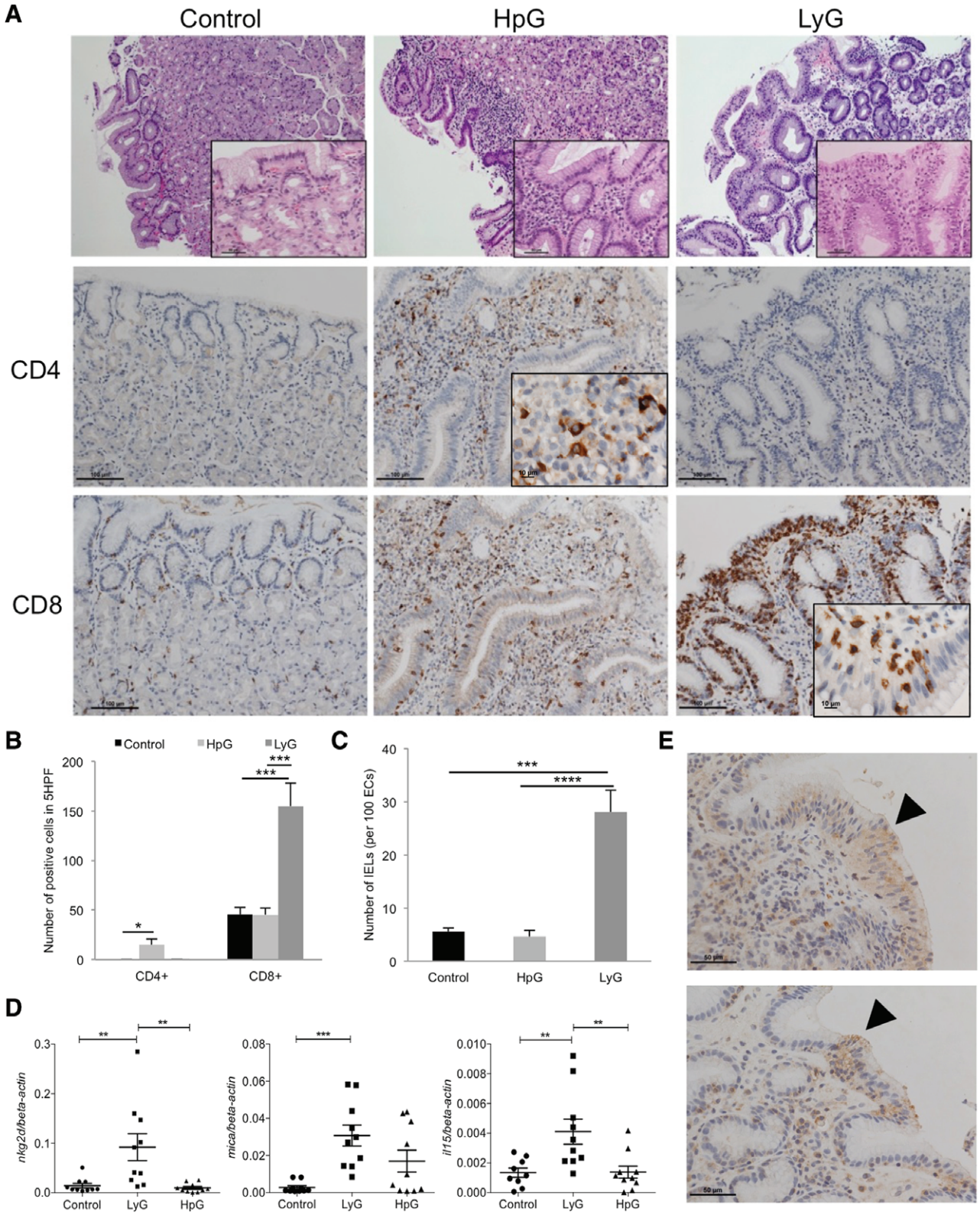

Figure 2. Immunophenotype and gene expression of the NKG2D–NKG2DL system and IL-15 in gastric corpus biopsies. (A) Haematoxylin and eosin and immunohistochemical staining of $CD4^+$ and $CD8^+$ T cells in human corpus biopsies of healthy controls, HpG cases, and LyG cases (overall magnification: upper panels, ×100; insets, ×400; middle and lower panels, ×200; immunohistochemistry insets, ×600). (B) IELs in LyG are $CD8^+$ and significantly enriched as compared with HpG and healthy controls. In HpG, $CD4^+$ cell numbers in the lamina propria are significantly increased as compared with LyG and healthy controls. (C) Number of IELs in healthy controls, HpG and LyG cases. (D) mRNA expression of *NKG2D*, *MICA* and *IL-15* indicates significant upregulation in LyG as compared with HpG and controls ($n = 10$ each). (E) Enhanced staining with a MICA/B antibody in gastric corpus biopsies of LyG cases in areas wherein IELs are more abundant (arrow) (magnification: ×400; $^*p < 0.05$, $^{**}p < 0.01$, $^{***}p < 0.001$, $^{****}p < 0.0001$; one-way ANOVA and Tukey's *post hoc* test).

Gastric epithelial cells respond to challenge with *P. acnes* and SCFAs by induction of NKG2D ligand expression, whereas *H. pylori* does not induce ligand expression

It has been shown that microbes are able to induce NKG2DL expression in certain cell lines; however, human gastric epithelia have not been investigated for their responsiveness thus far [17,18]. Therefore, we challenged AGS and MKN28 cells with *P. acnes* strains isolated from the human stomach, both *H. pylori* and *E. coli*, for 24 h (MOI of 1:50). After 24 h of challenge, *MICA*, *MICB* and *IL-15* expression was measured by RT-qPCR. Shorter co-culture times (4 h) did not substantially alter expression of the evaluated markers (supplementary material, Figure S4A). The growth of assessed strains determined by CFU plating was not significantly different after 24 h of co-cultures (supplementary material, Figure S4B). Live *P. acnes* significantly increased *MICA* and *MICB* mRNA levels in both gastric epithelial cell lines in a strain-dependent manner. For instance, strain PA2-2 consistently showed strong induction of ligand expression and also significantly induced *IL-15* mRNA expression, whereas PA1-1 significantly repressed *IL-15* expression. It is noteworthy that *H. pylori* strains SS1 and PMSS1 did not induce, but rather repressed, ligand and *IL-15* mRNA expression in both cell lines. The effect of *E. coli* challenge on mRNA levels was only minor as compared with *P. acnes* (Figure 3A–C).

It has been recently reported that SCFAs, including propionate derived from *P. acnes*, are potent inducers of NKG2DL expression [18]. SCFAs could be reliably detected in supernatants after a 24-h AGS challenge with *P. acnes* (supplementary material, Table S5). However, their concentration was approximately 1 to 2 log units lower than the concentration normally needed to reliably induce NKG2DL expression *in vitro* [18,47,48]. Thus, it is reasonable to speculate that other factors, such as direct bacterium–cell contact or other metabolites, also contributed to the observed induction of ligand expression in our challenge experiments [49]. To assess the net effect of propionate, and also the effect of the potent NKG2DL inducer butyrate, AGS and MKN28 cells were challenged with 5 mM SCFAs and HCl as a control for 4 h, and *MICA*, *MICB* and *IL-15* expression was assessed by RT-qPCR. Butyrate and propionate significantly induced *MICA* expression in both gastric epithelial cell lines and *MICB* expression in MKN28 cells. Both SCFAs also induced *IL-15* mRNA expression in AGS cells. MKN28 cells responded differently, showing no effect on *IL-15* mRNA expression or even repression. Neither acetate nor HCl changed the expression of ligands and *IL-15* mRNA in AGS cells, but repressed *IL-15* mRNA expression in MKN28 cells (Figure 3D–F).

It is of note that NKG2DL expression is differently regulated at the mRNA and protein levels [50]. Thus, we wanted to investigate whether challenge also translates into increased protein expression of NKG2DLs, which would be necessary for recruitment of NKG2D receptor-bearing lymphocytes to the ligand-overexpressing epithelium. By using flow cytometry and a MICA/B antibody, we found that challenge of AGS and MKN28 cells with live bacteria for 24 h (Figure 4A) or with 5 mM acetate, propionate, butyrate or HCl for 4 h (Figure 4B) did not alter overall ligand expression.

However, challenge experiments did show effects on extracellular ligand expression. *P. acnes* strains significantly induced extracellular MICA/B expression in both cell lines, whereas *H. pylori* strains did not alter (for AGS) or even repressed (for MKN28) extracellular MICA/B protein expression (Figure 4C). In addition, propionate and butyrate significantly increased extracellular MICA/B protein levels in both cell lines, whereas acetate and HCl did not alter (for AGS) or slightly repressed (for MKN28) extracellular MICA/B protein levels (Figure 4D). Taken together, these data indicate that live *P. acnes*, its main metabolite propionate and the SCFA butyrate are potent inducers ofNKG2DLs mRNA and extracellular protein expression, and also modulate *IL-15* mRNA levels in human gastric epithelial cells. Intriguingly, *H. pylori* does not induce, or even represses, mRNA and protein expression of NKG2DLs and IL-15.

Discussion

The pathogenesis of corpus-dominant LyG is so far unknown, but its responsiveness to antibiotic treatment suggests a bacterial trigger for disease development [6–8]. In this study, we subjected human stomach biopsies to comparative microbial community profiling, and found that *H. pylori* infection is not the cause of LyG, which is instead characterized by overabundance of *P. acnes*. Moreover, we found expression of the NKG2D–NKG2DL system and the proinflammatory cytokine IL-15 to be significantly induced in LyG, identifying the likely molecular determinants responsible for IEL recruitment, the typical phenotype represented by the disease. Finally, challenge of human gastric ECs with *P. acnes* and the microbial metabolites SCFAs revealed induction of NKG2DL expression, recapitulating the measurements found in human disease specimens. It is of note that *H. pylori* did not induce, or even repressed, NKG2DL expression.

Immune recognition mediated by the activating receptor NKG2D plays an important role in the elimination of stressed cells. NKG2DLs are expressed at low levels on epithelia under healthy conditions; however, their expression is greatly enhanced by factors causing cell stress, such as viral infection, heat shock, or neoplastic transformation [50,51]. In CeD, duodenal epithelia challenged with gliadin (i.e. the stressor) overexpress the NKG2DL MICA. In the presence of IL-15, cytotoxic $CD8^+$ lymphocytes expressing the activating receptor NKG2D are then recruited to the duodenal epithelium,

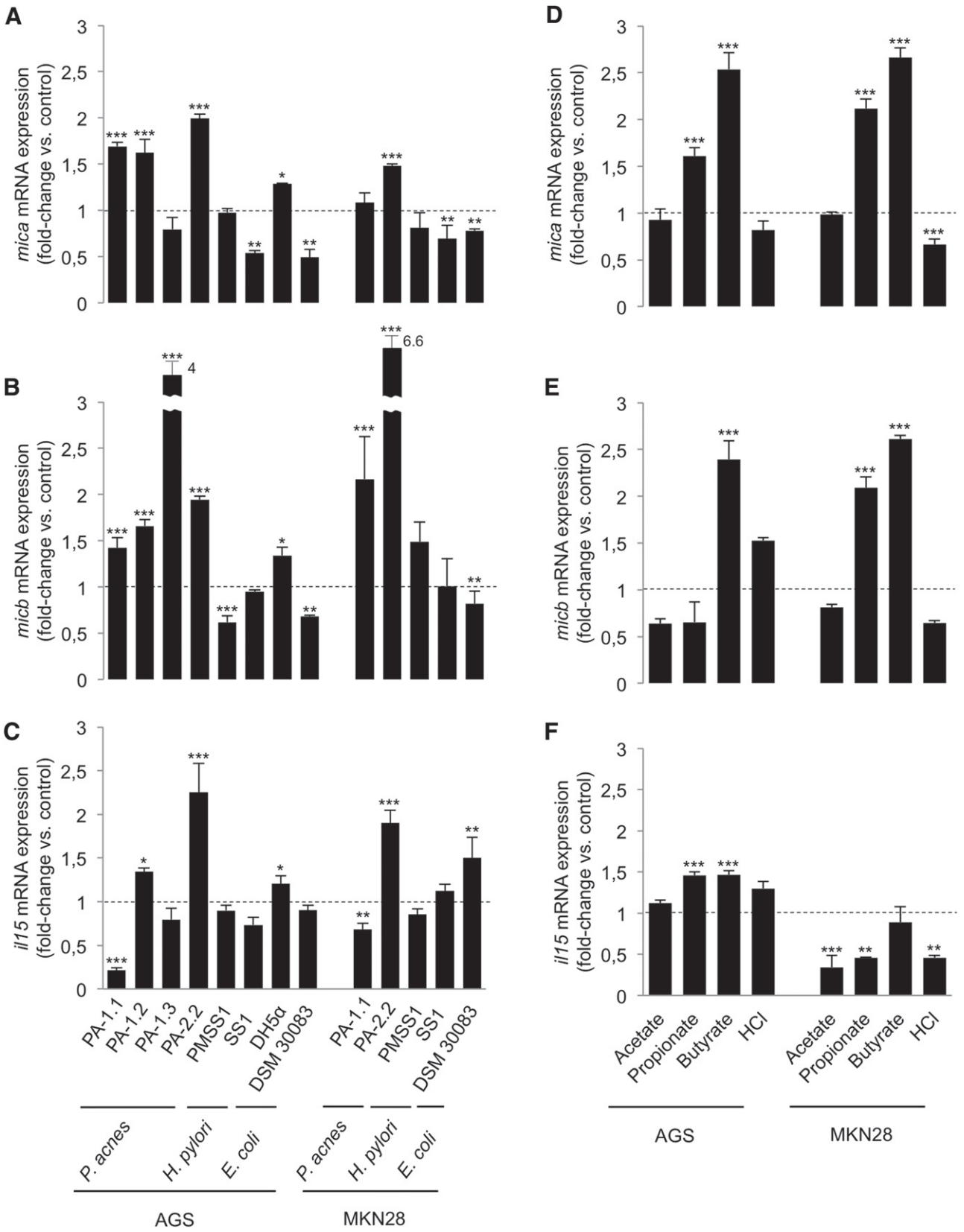

Figure 3. Gastric epithelial cells respond to *P. acnes* and SCFAs by induction of NKG2DL and *IL-15* mRNA expression, whereas *H. pylori* does not cause such induction. (A–C) AGS and MKN28 cells were infected with live bacteria for 24 h. *MICA* (A), *MICB* (B) and *IL-15* (C) mRNA relative abundance was measured by RT-qPCR. *P. acnes* strains isolated from the human stomach are able to induce NKG2DL expression in a strain-dependent manner, and had either inducing or repressing effects on *IL-15* expression. *H. pylori* challenge does not induce NKG2DL mRNA expresion or even represses transcription. (D–F) AGS and MKN28 cells were stimulated with 5 mM of different SCFAs and HCl (control). *MICA* (D), *MICB* (E) and *IL-15* (F) mRNA expression was assessed after 4 h of challenge. Propionate and butyrate induced NKG2DL expression in both cell lines. SCFAs had either inducing or repressing effects on *IL-15* mRNA transcript abundance, depending on the cell line (*$p < 0.05$; **$p < 0.01$; ***$p < 0.001$; one-way ANOVA and Dunnett's *post hoc* test).

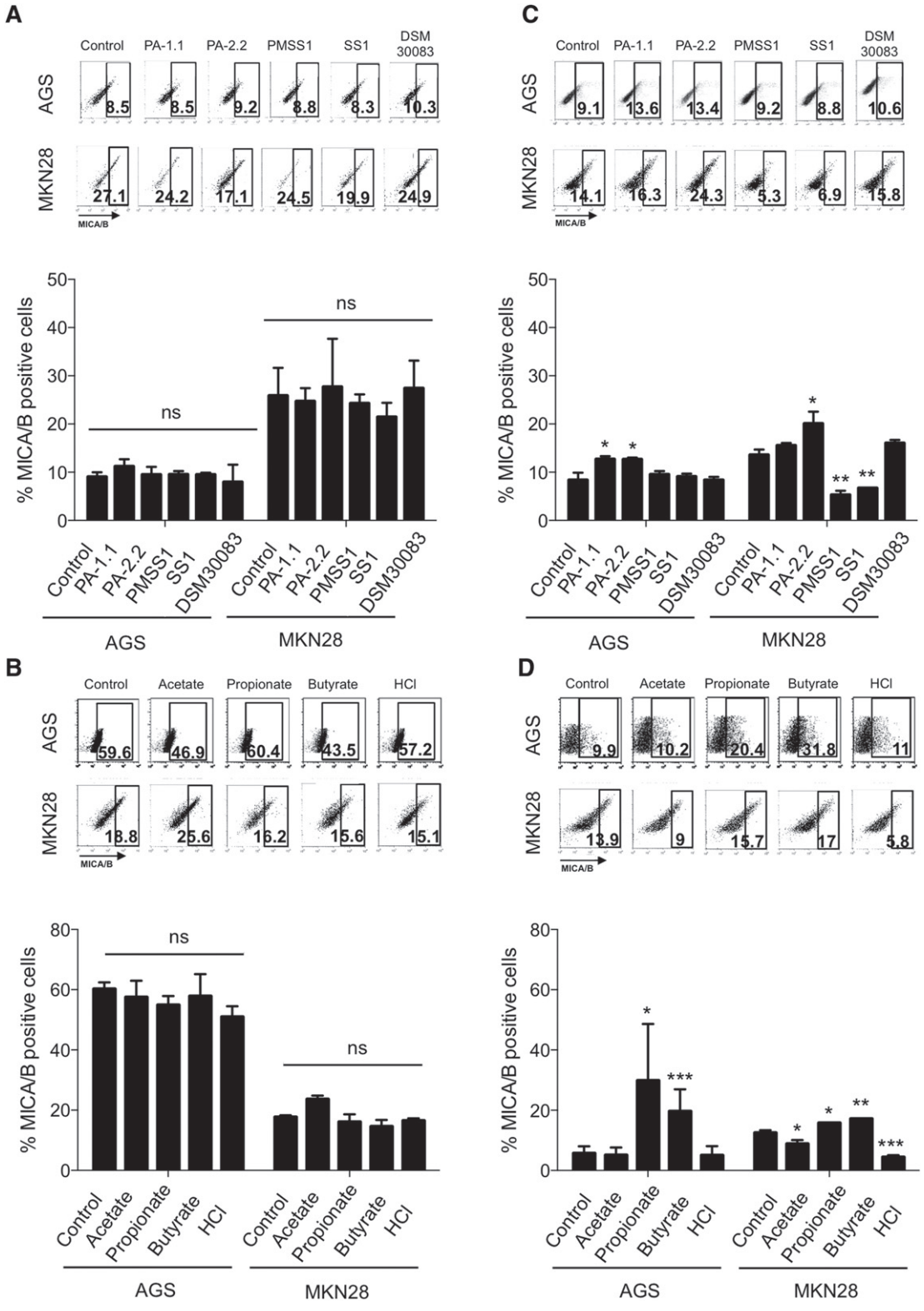

Figure 4. Gastric epithelial cells respond to *P. acnes* and SCFAs by induction of NKG2DL expression specifically on the cell surface, whereas *H. pylori* does not cause such induction. MICA/B protein expression was assessed in AGS and MKN28 cells by flow cytometry after challenge with bacteria for 24 h or SCFA stimulation for 4 h followed by 4 h of rescue in DMEM without SCFAs. Representative pictures of dot plots are shown at the top of each graph. (A) No change in overall MICA/B protein expression after bacterial challenge with *P. acnes*, *H. pylori* and *E. coli* strains. (B) No change in overall MICA/B protein expression after challenge with 5mM SCFAs and HCl (C) Significant induction of extracellular MICA/B protein expression after *P. acnes* challenge in AGS and MKN28 cells. *H. pylori* suppresses extracellular MICA/B expression in MKN28 cells. (D) Propionate and butyrate induce extracellular MICA/B protein; 10 000 events were analysed per readout. Readouts of concomitantly performed viability assays of AGS and MKN cells are shown in supplementary material, Figure S5. Bar charts represent the mean values of percentages of MICA/B-positive cells ± standard error of three independent experiments (*$p < 0.05$; **$p < 0.001$; ***$p < 0.0001$; one-way ANOVA and Dunnett's *post hoc* test). NS, not significant.

leading to the destruction of stressed cells via a cytotoxic T-cell response, which subsequently leads to villus atrophy, the hallmark lesion observed in CeD [9,10]. Recently, it has been shown that NKG2DL expression is modulated by the GI microbiota, either by direct microbe–cell interaction (e.g. via adherent *E. coli*) or by microbial products such as SCFAs [18,49]. Moreover, manipulation of the microbiota with antibiotics leads to either increased or decreased NKG2DL expression in mice, depending on the microbial spectra covered by the substance [17].

Historically, it has been considered that the stomach is a quasi-sterile environment, owing to its acidity, and that only bacteria with specific abilities (e.g. *H. pylori* with its urease production) are able to colonize this habitat. However, it has now become clear that the stomach's microbiota is quite diverse, and that it also contributes to the development of various gastric pathologies [44,45,52,53]. It is of note that *P. acnes*, a classic skin bacterium, has been recently identified as a part of the stomach microbiota [43,52,54,55]. By the use of culture-dependent and culture-independent techniques, *P. acnes* was found to be a member of the stomach microbiota in healthy individuals, representing >20% of microbes in certain cases [55]. Interestingly, *P. acnes* was found only in mucosal specimens and not in the gastric fluid, indicating the preferred niche of this bacterium [56]. Whether specific pathotypes of *P. acnes* contribute to LyG development, or whether the increase in the abundance of *P. acnes* over a certain level is itself sufficient to induce NKG2DL overexpression, is not known so far, and should be a focus for future investigations. Nevertheless, *P. acnes* is able to resist acid stress, and it shows a variety of virulence mechanisms, which could contribute to inflammation, epithelial cell stress, and ultimately to NKG2D–NKG2DL activation [34,57–62]. Interestingly, in HpG (a condition certainly favouring cell stress of gastric epithelia, owing to its prominent inflammation), neither NKG2D nor MICA or IL-15 expression were found to be induced. In contrast, we noted only slight induction of MICB expression in biopsies. Moreover, *H. pylori* failed to induce or even impaired mRNA and extracellular protein expression in challenge experiments with gastric epithelial cells. Importantly, the NKG2D–NKG2DL system and IL-15 are important for tumour surveillance, which is necessary for the elimination of neoplastic cells [63]. The system has therefore been investigated as a potent target for cancer immunotherapy in various studies [64–68]. From our data, it could be speculated that *H. pylori* does not have the ability to activate the NKG2D–NKG2DL system, and this might eventually favour stomach cancer development as a long-term sequel of *H. pylori* infection, because of impaired innate antitumour immunity. The downregulation of *IL-15* in HpG has also been reported recently [69]. Thus investigating the NKG2D–NKG2DL system in the context of HpG and gastric adenocarcinoma development should be a reasonable future research aim.

In conclusion, our study identifies the NKG2D–NKG2DL system and the proinflammatory cytokine IL-15 as likely molecular players in corpus-dominant LyG. Thus, similarities between LyG and the paradigm disease of intraepithelial lymphocytosis, CeD, also exist at the molecular level. The identified increase in *P. acnes* abundance in LyG possibly contributes to pathogenesis, as also shown by the *in vitro* cell challenge experiments. Identifying the causes leading to *P. acnes* overgrowth or which additional factors contribute to NKG2D–NKG2DL and IL-15 activation should initiate prospective studies investigating LyG. This would enable, for instance, genotyping and phenotyping of *P. acnes* isolates from cases, which is not feasible with archived FFPE material.

Author contributions statement

The authors contributed in the following way: GG, CL, AM-A: conceptualization and methodology; AM-A, PW, ST, SS, GG: investigation and formal analysis; GG, AM-A: writing of original draft; AM-A, PW, ST, BH, SK, CH, GG: writing, review and editing; GG: funding acquisition; GG, CH, BH: resources; GG: supervision.

Acknowledgements

We are grateful to B Mayo and MJ Blaser for providing *P. acnes* and *H. pylori* strains, respectively, S Wessler for providing gastric epithelial cell lines, and J Krysl, N Madhusudhan, L Preiss, I Klymiuk, M Trötzmüller and H Köfeler for their technical support. JC Becker and J Galindo-Villegas are acknowledged for helpful discussions and their thesis committee contributions, and W Florian Fricke for his input to the manuscript. The work was supported by the Austrian Science Fund (FWF W1241-B18), BioTechMed Graz and the Medical University of Graz (DK-MOLIN).

References

1. Wu TT, Hamilton SR. Lymphocytic gastritis: association with etiology and topology. *Am J Surg Pathol* 1999; **23:** 153–158.
2. Vakiani E, Yantiss RK. Lymphocytic gastritis: clinicopathologic features, etiologic associations, and pathogenesis. *Pathol Case Rev* 2008; **13:** 167–171.
3. Lynch DA, Sobala GM, Dixon MF, *et al.* Lymphocytic gastritis and associated small bowel disease: a diffuse lymphocytic gastroenteropathy? *J Clin Pathol* 1995; **48:** 939–945.
4. Oberhuber G, Bodingbauer M, Mosberger I, *et al.* High proportion of granzyme B-positive (activated) intraepithelial and lamina propria lymphocytes in lymphocytic gastritis. *Am J Surg Pathol* 1998; **22:** 450–458.
5. Nielsen JA, Roberts CA, Lager DJ, *et al.* Lymphocytic gastritis is not associated with active Helicobacter pylori infection. Helicobacter 2014; **19:** 349–355.

6. Müller H, Volkholz H, Stolte M. Healing of lymphocytic gastritis by eradication of Helicobacter pylori. *Digestion* 2001; **63:** 14–19.
7. Hayat M, Arora DS, Dixon MF, *et al.* Effects of Helicobacter pylori eradication on the natural history of lymphocytic gastritis. *Gut* 1999; **45:** 495–498.
8. Madisch A, Miehlke S, Neuber F, *et al.* Healing of lymphocytic gastritis after Helicobacter pylori eradication therapy – a randomized, double-blind, placebo-controlled multicentre trial. *Aliment Pharmacol Ther* 2006; **23:** 473–479.
9. Meresse B, Chen Z, Ciszewski C, *et al.* Coordinated induction by IL15 of a TCR-independent NKG2D signaling pathway converts CTL into lymphokine-activated killer cells in celiac disease. *Immunity* 2004; **21:** 357–366.
10. Hue S, Mention JJ, Monteiro RC, *et al.* A direct role for NKG2D/MICA interaction in villous atrophy during celiac disease. *Immunity* 2004; **21:** 367–377.
11. Raulet DH, Gasser S, Gowen BG, *et al.* Regulation of ligands for the NKG2D activating receptor. *Annu Rev Immunol* 2013; **31:** 413–441.
12. Allez M, Tieng V, Nakazawa A, *et al.* CD4+NKG2D+ T cells in Crohn's disease mediate inflammatory and cytotoxic responses through MICA interactions. *Gastroenterology* 2007; **132:** 2346–2358.
13. Guerra N, Pestal K, Juarez T, *et al.* A selective role of NKG2D in inflammatory and autoimmune diseases. *Clin Immunol* 2013; **149:** 432–439.
14. Bauer S, Groh V, Wu J, *et al.* Activation of NK cells and T cells by NKG2D, a receptor for stress-inducible MICA. *Science* 1999; **285:** 727–729.
15. Kasahara M, Yoshida S. Immunogenetics of the NKG2D ligand gene family. *Immunogenetics* 2012; **64:** 855–867.
16. Pagliari D, Cianci R, Frosali S, *et al.* The role of IL-15 in gastrointestinal diseases: a bridge between innate and adaptive immune response. *Cytokine Growth Factor Rev* 2013; **24:** 455–466.
17. Hansen CH, Holm TL, Krych L, *et al.* Gut microbiota regulates NKG2D ligand expression on intestinal epithelial cells. *Eur J Immunol* 2012; **43:** 447–457.
18. Andresen L, Hansen KA, Jensen H, *et al.* Propionic acid secreted from propionibacteria induces NKG2D ligand expression on human-activated T lymphocytes and cancer cells. *J Immunol* 2009; **183:** 897–906.
19. Cutler AF, Havstad S, Ma CK, *et al.* Accuracy of invasive and noninvasive tests to diagnose Helicobacter pylori infection. *Gastroenterology* 1995; **109:** 136–141.
20. Liu Z, DeSantis TZ, Andersen GL, *et al.* Accurate taxonomy assignments from 16S rRNA sequences produced by highly parallel pyrosequencers. *Nucleic Acids Res* 2008; **36:** e120.
21. Gorkiewicz G, Thallinger GG, Trajanoski S, *et al.* Alterations in the colonic microbiota in response to osmotic diarrhea. *PLoS One* 2013; **8:** e55817.
22. Schloss PD, Gevers D, Westcott SL. Reducing the effects of PCR amplification and sequencing artifacts on 16S rRNA-based studies. *PLoS One* 2011; **6:** e27310.
23. Quince C, Lanzen A, Curtis TP, *et al.* Accurate determination of microbial diversity from 454 pyrosequencing data. *Nat Methods* 2009; **6:** 639–641.
24. Huse SM, Welch DM, Morrison HG, *et al.* Ironing out the wrinkles in the rare biosphere through improved OTU clustering. *Environ Microbiol* 2010; **12:** 1889–1898.
25. Edgar RC, Haas BJ, Clemente JC, *et al.* UCHIME improves sensitivity and speed of chimera detection. *Bioinformatics* 2011; **27:** 2194–2200.
26. Wang Q, Garrity GM, Tiedje JM, *et al.* Naive Bayesian classifier for rapid assignment of rRNA sequences into the new bacterial taxonomy. *Appl Environ Microbiol* 2007; **73:** 5261–5267.
27. Quast C, Pruesse E, Yilmaz P, *et al.* The SILVA ribosomal RNA gene database project: improved data processing and web-based tools. *Nucleic Acids Res* 2013; **41:** D590–D596.
28. Pruesse E, Quast C, Knittel K, *et al.* SILVA: a comprehensive online resource for quality checked and aligned ribosomal RNA sequence data compatible with ARB. *Nucleic Acids Res* 2007; **35:** 7188–7196.
29. Caporaso JG, Kuczynski J, Stombaugh J, *et al.* QIIME allows analysis of high-throughput community sequencing data. *Nat Methods* 2010; **7:** 335–336.
30. Edgar RC. Search and clustering orders of magnitude faster than BLAST. *Bioinformatics* 2010; **26:** 2460–2461.
31. Segata N, Izard J, Waldron L, *et al.* Metagenomic biomarker discovery and explanation. *Genome Biol* 2011; **12:** R60.
32. Lozupone C, Lladser ME, Knights D, *et al.* UniFrac: an effective distance metric for microbial community comparison. *ISME J* 2011; **5:** 169–172.
33. Pfaffl MW. A new mathematical model for relative quantification in real-time RT-PCR. *Nucleic Acids Res* 2001; **29:** 2002–2007.
34. Delgado S, Suarez A, Mayo B. Identification, typing and characterisation of Propionibacterium strains from healthy mucosa of the human stomach. *Int J Food Microbiol* 2011; **149:** 65–72.
35. Thompson LJ, Danon SJ, Wilson JE, *et al.* Chronic Helicobacter pylori infection with Sydney strain 1 and a newly identified mouse-adapted strain (Sydney strain 2000) in C57BL/6 and BALB/c mice. *Infect Immun* 2004; **72:** 4668–4679.
36. Lee A, O'Rourke J, De Ungria MC, *et al.* A standardized mouse model of Helicobacter pylori infection: introducing the Sydney strain. *Gastroenterology* 1997; **112:** 1386–1397.
37. Woodcock DM, Crowther PJ, Doherty J, *et al.* Quantitative evaluation of Escherichia coli host strains for tolerance to cytosine methylation in plasmid and phage recombinants. *Nucleic Acids Res* 1989; **17:** 3469–3478.
38. Schneider S, Carra G, Sahin U, *et al.* Complex cellular responses of Helicobacter pylori-colonized gastric adenocarcinoma cells. *Infect Immun* 2011; **79:** 2362–2371.
39. Tazoe H, Otomo Y, Kaji I, *et al.* Roles of short-chain fatty acids receptors, GPR41 and GPR43 on colonic functions. *J Physiol Pharmacol* 2008; **59**(suppl 2)**:** 251–262.
40. Alva-Murillo N, Ochoa-Zarzosa A, Lopez-Meza JE. Short chain fatty acids (propionic and hexanoic) decrease Staphylococcus aureus internalization into bovine mammary epithelial cells and modulate antimicrobial peptide expression. *Vet Microbiol* 2012; **155:** 324–331.
41. Iraporda C, Errea A, Romanin DE, *et al.* Lactate and short chain fatty acids produced by microbial fermentation downregulate proinflammatory responses in intestinal epithelial cells and myeloid cells. *Immunobiology* 2015; **220:** 1161–1169.
42. Clayton A, Mitchell JP, Court J, *et al.* Human tumor-derived exosomes down-modulate NKG2D expression. *J Immunol* 2008; **180:** 7249–7258.
43. Monstein HJ, Tiveljung A, Kraft CH, *et al.* Profiling of bacterial flora in gastric biopsies from patients with Helicobacter pylori-associated gastritis and histologically normal control individuals by temperature gradient gel electrophoresis and 16S rDNA sequence analysis. *J Med Microbiol* 2000; **49:** 817–822.
44. Bik EM, Eckburg PB, Gill SR, *et al.* Molecular analysis of the bacterial microbiota in the human stomach. *Proc Natl Acad Sci USA* 2006; **103:** 732–737.
45. Maldonado-Contreras A, Goldfarb KC, Godoy-Vitorino F, *et al.* Structure of the human gastric bacterial community in relation to Helicobacter pylori status. *ISME J* 2011; **5:** 574–579.
46. Li X-X, Wong GL-H, To K-F, *et al.* Bacterial microbiota profiling in gastritis without Helicobacter pylori infection or non-steroidal anti-inflammatory drug use. *PLoS One* 2009; **4:** e7985.

47. Gamet L, Daviaud D, Denis-Pouxviel C, *et al.* Effects of short-chain fatty acids on growth and differentiation of the human colon-cancer cell line HT29. *Int J Cancer* 1992; **52:** 286–289.
48. Engelmann GL, Staecker JL, Richardson AG. Effect of sodium butyrate on primary cultures of adult rat hepatocytes. *In Vitro Cell Dev Biol* 1987; **23:** 86–92.
49. Tieng V, Le Bouguénec C, du Merle L, *et al.* Binding of Escherichia coli adhesin AfaE to CD55 triggers cell-surface expression of the MHC class I-related molecule MICA. *Proc Natl Acad Sci USA* 2002; **99:** 2977–2982.
50. Raulet DH. Roles of the NKG2D immunoreceptor and its ligands. *Nat Rev Immunol* 2003; **3:** 781–790.
51. Groh V, Bahram S, Bauer S, *et al.* Cell stress-regulated human major histocompatibility complex class I gene expressed in gastrointestinal epithelium. *Proc Natl Acad Sci USA* 1996; **93:** 12445–12450.
52. Yang I, Nell S, Suerbaum S. Survival in hostile territory: the microbiota of the stomach. *FEMS Microbiol Rev* 2013; **37:** 736–761.
53. Lofgren JL, Whary MT, Ge Z, *et al.* Lack of commensal flora in Helicobacter pylori-infected INS-GAS mice reduces gastritis and delays intraepithelial neoplasia. *Gastroenterology* 2011; **140:** 210–220.
54. Zilberstein B, Quintanilha AG, Santos MA, *et al.* Digestive tract microbiota in healthy volunteers. *Clinics (Sao Paulo)* 2007; **62:** 47–54.
55. Delgado S, Cabrera-Rubio R, Mira A, *et al.* Microbiological survey of the human gastric ecosystem using culturing and pyrosequencing methods. *Microb Ecol* 2013; **65:** 763–772.
56. von Rosenvinge EC, Song Y, White JR, *et al.* Immune status, antibiotic medication and pH are associated with changes in the stomach fluid microbiota. *ISME J* 2013; **7:** 1354–1366.
57. Brzuszkiewicz E, Weiner J, Wollherr A, *et al.* Comparative genomics and transcriptomics of Propionibacterium acnes. *PLoS One* 2011; **6:** e21581.
58. Lodes MJ, Secrist H, Benson DR, *et al.* Variable expression of immunoreactive surface proteins of Propionibacterium acnes. *Microbiology* 2006; **152:** 3667–3681.
59. Holland C, Mak TN, Zimny-Arndt U, *et al.* Proteomic identification of secreted proteins of Propionibacterium acnes. *BMC Microbiol* 2010; **10:** 230.
60. Mak TN, Fischer N, Laube B, *et al.* Propionibacterium acnes host cell tropism contributes to vimentin-mediated invasion and induction of inflammation. *Cell Microbiol* 2012; **14:** 1720–1733.
61. Nakatsuji T, Tang DC, Zhang L, *et al.* Propionibacterium acnes CAMP factor and host acid sphingomyelinase contribute to bacterial virulence: potential targets for inflammatory acne treatment. *PLoS One* 2011; **6:** e14797.
62. Tomida S, Nguyen L, Chiu BH, *et al.* Pan-genome and comparative genome analyses of propionibacterium acnes reveal its genomic diversity in the healthy and diseased human skin microbiome. *MBio* 2013; **4:** e00003–e00013.
63. Guerra N, Tan YX, Joncker NT, *et al.* NKG2D-deficient mice are defective in tumor surveillance in models of spontaneous malignancy. *Immunity* 2008; **28:** 571–580.
64. Coudert JD, Held W. The role of the NKG2D receptor for tumor immunity. *Semin Cancer Biol* 2006; **16:** 333–343.
65. Nausch N, Cerwenka A. NKG2D ligands in tumor immunity. *Oncogene* 2008; **27:** 5944–5958.
66. Lopez-Soto A, Huergo-Zapico L, Acebes-Huerta A, *et al.* NKG2D signaling in cancer immunosurveillance. *Int J Cancer* 2015; **136:** 1741–1750.
67. El-Gazzar A, Groh V, Spies T. Immunobiology and conflicting roles of the human NKG2D lymphocyte receptor and its ligands in cancer. *J Immunol* 2013; **191:** 1509–1515.
68. Waldmann TA. The biology of interleukin-2 and interleukin-15: implications for cancer therapy and vaccine design. *Nat Rev Immunol* 2006; **6:** 595–601.
69. Luzza F, Parrello T, Monteleone G, *et al.* Changes in the mucosal expression of interleukin 15 in Helicobacter pylori-associated gastritis. *FEMS Immunol Med Microbiol* 1999; **24:** 233–238.

SUPPLEMENTARY MATERIAL ONLINE

Supplementary materials and methods

Supplementary figure legends

Figure S1. Differences at phylum level between healthy controls, HpG and LyG.

Figure S2. Validation of NGS sequencing results by qPCR.

Figure S3. NKG2DL expression in corpus biopsies measured by qRT-PCR.

Figure S4. AGS cell challenge for 4 h and bacterial viable cell counts.

Figure S5. Apoptosis and live/dead staining assay.

Table S1. Sample information, metadata and analyses performed.

Table S2. Primers used in this study.

Table S3. Richness, diversity, evenness.

Table S4. LEfSe analysis output.

Table S5. Concentration of SCFAs in the supernatant of challenged AGS cells.